

Analysis of Fluorescence Collection Efficiency for Fiber-optic Scanning Two-photon Endomicroscopy

Conghao Wang^a, Huilan Liu^{a,b}, Aimin Wang^c and Lishuang Feng^{*a,b,d}

^aSchool of Instrumentation and Optoelectronic Engineering, Beihang University, Beijing 100191, China; ^bKey Laboratory of Precision Opto-Mechatronics Technology (Ministry of Education), Beijing 100191, China; ^cState Key Laboratory of Advanced Optical Communication System and Networks, School of Electronics, Peking University, Beijing 100871, China; ^dLaboratory of Intelligent Sensing Materials and Chip Integration Technology of Zhejiang Province, Hangzhou innovation institute of Beihang University, Hangzhou 310063, China

ABSTRACT

Piezoelectric ceramic tube fiber-scanning two-photon endomicroscopy is an essential division of miniature two-photon microscopy. The reverse collection optical path of the two-photon endomicroscopy platform is modeled and designed in this study. After simulating the chromatic aberration characteristics of the objective, the effects of the collection signal wavelengths, off-axis positions, fiber cladding diameters, and imaging depths on the collection efficiency are evaluated using Monte Carlo simulation. The results provide an additional theoretical explanation for enhancing the two-photon endomicroscopy platform's imaging sensitivity and signal-to-noise ratio.

Keywords: two-photon endomicroscopy, collection efficiency, double-cladding fiber, piezoelectric ceramic scanning

1. Introduction

Two-photon microscopy is a significant imaging tool designed for visualizing living tissue with subcellular resolution [1], and this technique provide greater imaging depth than single-photon microscopy due to its second-order nonlinear excitation effect. Advancements in nonlinear miniature microscopy enable imaging of the structures and functions of animal organs under freely-behaving conditions [2-4].

Many research groups have developed fiber-scanning two-photon endomicroscopy (TPEM) as a promising application of miniature two-photon microscopy [5-7]. This common-path nonlinear imaging method drives a resonant double-cladding fiber (DCF) with a piezoelectric ceramic tube (PZT), thereby enabling two-dimensional (Lissajous, spiral, raster) scanning. The DCF is the core optical transmission component of the TPEM, which has a dual-transmission function; the fiber core transmits femtosecond pulses, while the fiber cladding transmits fluorescence signals. The TPEM's excitation source is a near-infrared wavelength femtosecond laser source, and the visible fluorescence signal is collected in the reverse direction. The inability of conventional gradient-index (GRIN) lenses to eliminate chromatic aberration is a significant limitation. The chromatic aberration in TPEM results in a larger focal shift, which reduces the fiber cladding's capacity to collect fluorescence signals to their fullest capacity.

In this study, we analyzed fluorescence collection efficiency using the TPEM platform developed by our research group [8-9]. We investigated the chromatic aberration properties of the miniaturized objective and the effects of collection signal wavelengths, off-axis positions, cladding diameters, and imaging depths on collection efficiency by Monte Carlo analysis. The TPEM imaging results for the gastric wall section are also presented.

*fenglishuang@buaa.edu.cn

2. Theoretical Analysis

Fig. 1 (a) depicts the optical collection path of the fiber-scanning TPTEM based on DCF. Due to chromatic aberration, the reverse fluorescence signal is focused in front of the DCF end, and the distance between these two points is known as the focal shift. Varying focus shifts for different wavelengths explain the differences in collection efficiency. Fig. 1 (b) depicts the optical path configuration of the miniaturized objective we utilized, which has working distance (WD) of 150 μm , an image side numerical aperture of 0.6, and a magnification of $3\times$ [10]. To collect two-photon excited fluorescence signals, we used a double-cladding antiresonant fiber (DC-ARF) with a cladding diameter of 13 μm .

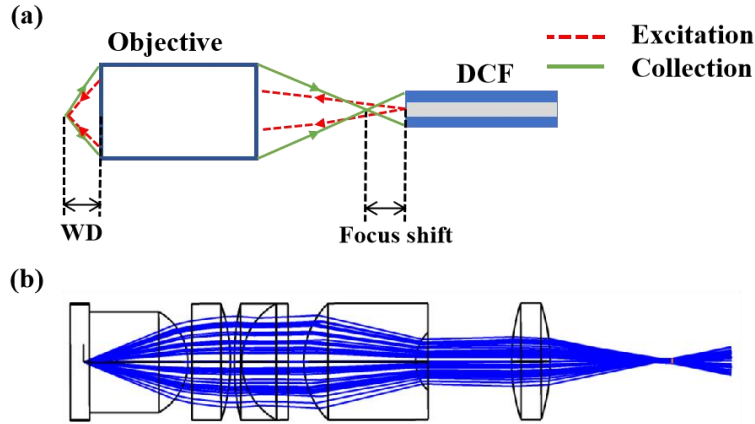


Fig. 1. (a) Schematic of TPTEM collection optical path; (b) objective structure.

Fig. 2 depicts the focal shifts of the objective corresponding to the various wavelengths, demonstrating that as the emission fluorescence wavelength decreases, the corresponding focal shift increases. The focal point shift is 353.7 μm when the fluorescence collection wavelength is 500 nm. Moreover, the focal point shift is 443.1 μm when the fluorescence collection wavelength is 450 nm.

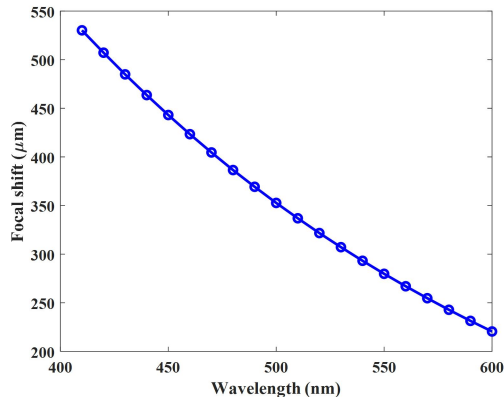


Fig. 2. Simulation of objective focal shifts.

In most biological tissues, light scattering is often stronger, and light absorption can be neglected [11]. The non-sequential reverse collection model is designed and analyzed by Zemax OpticStudio. The scattering coefficient μ_s and scattering anisotropy parameter g at different wavelengths are set with reference to Ref. 12, and the specific values can be found in Table 1. Using the Monte Carlo analysis tool, we evaluated and analyzed the reverse fluorescence collection efficiency of the TPTEM platform. When the detection surface radius (or cladding radius) is set to 0.067 mm, Fig. 3 (a) demonstrates that an increase in chromatic aberration causes larger focal shifts, thereby decreasing the normalized collection intensity. We placed the point source and detection surface in various off-axis positions to simulate the variation in normalized collection intensity under different fields of view during fiber cantilever scanning. Fig. 3 (b) depicts the simulation results, where 400 nm collection wavelengths have greater off-axis effect on the normalized collection intensity.

Table 1. Scattering parameters used in the simulation.

Parameter	Wavelength	400 nm	450 nm	500 nm	550 nm	600 nm
μ_a (cm ⁻¹)		42.6	39.4	34.7	31.9	28.7
g		0.937	0.94	0.943	0.948	0.953

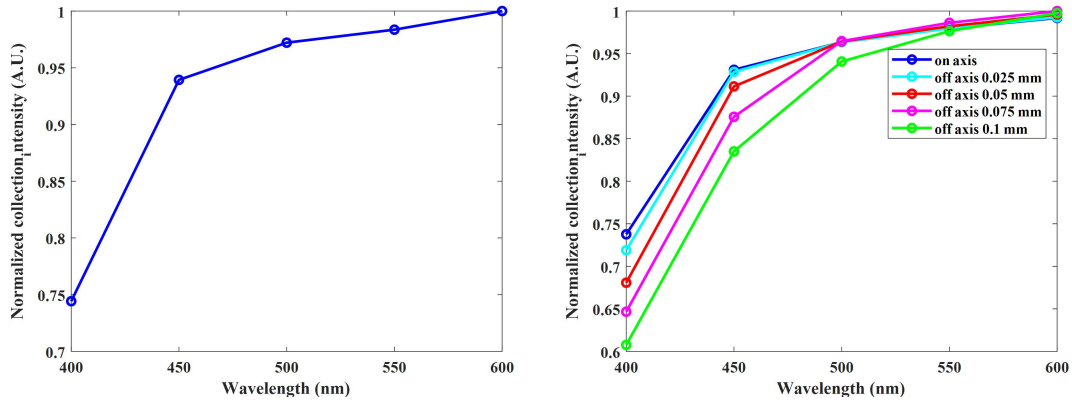


Fig. 3. (a) Simulation of normalized collection intensity versus collection wavelength; (b) Simulations of normalized collection intensity versus different off-axis positions.

The effects of fiber cladding radius values of 0.05 mm, 0.067 mm, 0.1 mm, 0.15 mm, and 0.2 mm on the normalized collection intensity are simulated, and the results are depicted in Fig. 4 (a). When the cladding radius is greater than 0.1 mm, the normalized fluorescence collection intensity at 400 nm~600 nm is greater than 0.9. Fig. 4 (b) shows that the normalized collection intensity results in different wavelengths and depths. In other words, as imaging depth increases, more photons are scattered, resulting in a decline in fluorescence collection efficiency.

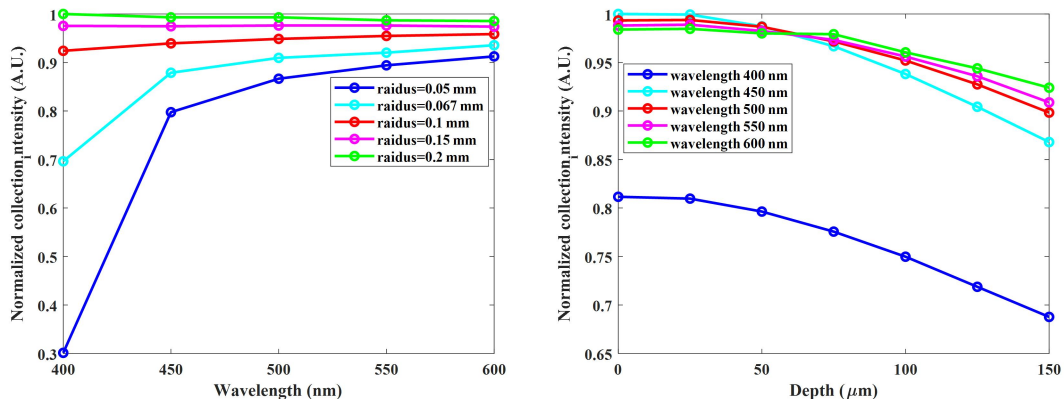


Fig. 4. (a) Simulations of normalized collection intensity versus different detection surface radius; (b) Simulations of normalized collection intensity versus different depths and wavelengths.

3. Imaging Results

The TPDM platform based on the DC-ARF and 3× objectives is shown in Fig. 5. Our previous work provides additional experimental details [8-9]. The assembled probe has an outer diameter of 5.8 mm and a rigid length of 49.1 mm. Fig. 6

shows the results of two-photon imaging of stained gastric wall sections (No. 61, Bresser Prepared Slides, 100 pcs), revealing the glandular structure of the gastric wall.

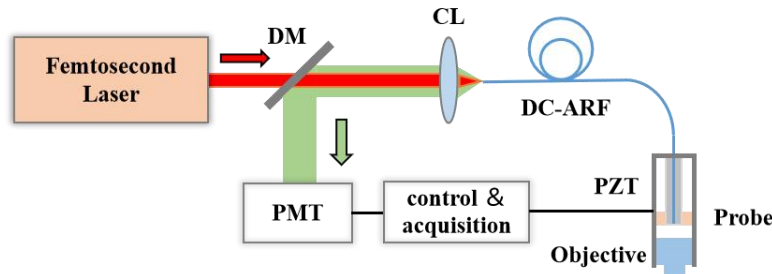


Fig. 5. TPEM setup.

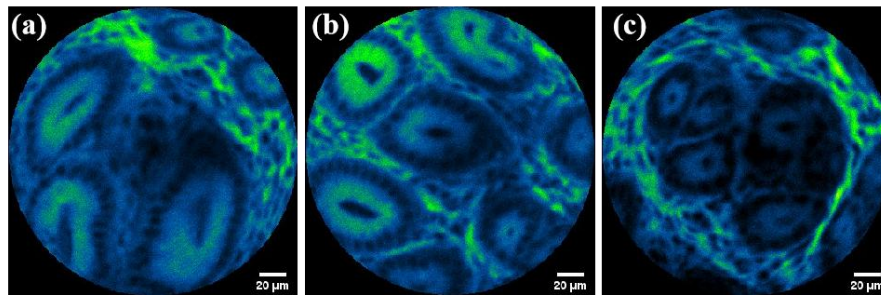


Fig. 6. Imaging results of gastric walls by TPEM.

4. Conclusion

In this study, the collection efficiency of the fiber-scanning two-photon endomicroscopy was modeled and analyzed. We used Monte Carlo analysis to examine the chromatic aberration properties of the miniaturized objective and how collection wavelengths, off-axis positions, cladding diameters, and imaging depths affected collection efficiency. Finally, the TPEM imaging results of stained gastric wall sections were shown. This work can provide a theoretical basis for improving the imaging sensitivity and signal-to-noise ratio of the two-photon endomicroscopy platform.

References

- [1] W. R. Zipfel, R. M. Williams, and W. W. Webb, "Nonlinear magic: multiphoton microscopy in the biosciences," *Nat. Biotechnol.* 21(11), 1369–1377 (2003).
- [2] F. Helmchen, M. S. Fee, D. W. Tank, and W. Denk, "A miniature head-mounted two-photon microscope: High-resolution brain imaging in freely moving animals," *Neuron* 31(6), 903–912 (2001).
- [3] Klioutchnikov, D. J. Wallace, M. H. Frosz, R. Zeltner, J. Sawinski, V. Pawlak, K. M. Voit, P. St. J. Russell, and J. N. D. Kerr, "Three-photon head-mounted microscope for imaging deep cortical layers in freely moving rats," *Nat. Methods.* 17(5), 509-513 (2020).
- [4] W. Zong, R. Wu, S. Chen, J. Wu, H. Wang, Z. Zhao, G. Chen, R. Tu, D. Wu, Y. Hui, Y. Xu, Y. Wang, Z. Duan, H. Wu, Y. Zhang, J. Zhang, A. Wang, L. Chen, and H. Cheng, "Miniature two-photon microscopy for enlarged field-of-view, multi-plane and long-term brain imaging," *Nat. Methods.* 18(1), 46-49 (2021).
- [5] M. T. Myaing, D. J. Macdonald, and X. Li. "Fiber-optic scanning two-photon fluorescence endoscope," *Opt. Lett.* 31(8), 1076–1077 (2006).
- [6] D. Septier, V. Mytskaniuk, R. Habert, D. Labat, K. Baudelle, A. Cassez, G. Brévalle-Wasilewski, M. Conforti, G. Bouwmans, H. Rigneault, and A. Kudlinski, "Label-free highly multimodal nonlinear endoscope," *Opt. Express* 30(14), 25020-25033 (2022).
- [7] D. Y. Kim, K. Hwang, J. Ahn, Y. H. Seo, J. B. Kim, S. Lee, J. H. Yoon, E. Kong, Y. Jeong, S. Jon, P. Kim, and K. H. Jeong, "Lissajous scanning two-photon endomicroscope for in vivo tissue imaging," *Sci. Rep.* 9, 3560 (2019).
- [8] C. Wang, H. Liu, J. Ma, H. Cui, Y. Li, D. Wu, Y. Hu, D. Wu, Q. Fu, L. Liang, F. Yu, R. Wu, A. Wang, and L. Feng, "Spiral scanning fiber-optic two-photon endomicroscopy with a double-cladding antiresonant fiber," *Opt. Express* 29(26), 43124–43135 (2021).

- [9] C. Wang, H. Liu, J. Ma, H. Cui, J. Tian, Q. Fu, R. Wu, A. Wang, and L. Feng, "Flexible two-photon endomicroscope probe with double-cladding antiresonant fiber," *Imaging Systems and Applications*. Optica Publishing Group, 2022, JW2A. 21.
- [10] D. Wu, L. Feng, and A. Wang, "Optical design of two-photon endoscopy objective with high collection efficiency," *Laser Optoelectron. Prog.* 55(07), 400–405 (2018).
- [11] F. Helmchen and W. Denk, "Deep tissue two-photon microscopy," *Nat. Methods* 2(12), 932–940 (2005).
- [12] Y. Wu, and X. Li, "Combined influences of chromatic aberration and scattering in depth-resolved two-photon fluorescence endospectroscopy," *Biomed. Opt. Express*, 1(4), 1234-1243 (2010).